Version 1.1: December 3, 1999
Position of gating grid fixed
in Fig. 2; caption clarified.

Version 1.0: September 3, 1999

STAR Note 408

STAR TPC: Review of the Fields and Electron Drift in P10 in the Gating-Grid/Anode-Wire Region

R. Bossingham, I. Sakrejda and T. Trainor

The overall electron drift time from the STAR TPC cathode (central membrane) to one anode wire readout is regulated automatically; the HV system (Univ. of Washington) uses a feedback loop controlling the cathode potential. Electron drift velocities are nearly constant from cathode to gating grid, but vary from there to the anode wire. The velocities in the latter region differ slightly between the inner and outer subsectors, and the cathode-anode plane separation is also 0.2 cm more for the outer subsector.

If, in contrast to the physical detection (anode-wire) planes at $Z_{\mathrm{d,in}}$ and $Z_{\mathrm{d,out}}$, two "effective detection planes" are defined at $Z'_{\mathrm{d,in}}$ and $Z'_{\mathrm{d,out}}$—conceptually independent of the channel-to-channel variations of FEE timing and overall trigger delay—the drift velocity can usually be treated as a constant. $Z'_{\mathrm{d,out}}$ and $Z'_{\mathrm{d,in}}$ are estimated using the GARFIELD drift code for this Note, then compared to experimental values.

In this context, the electric fields in the gating-grid/anode-wire regions of the STAR TPC are reviewed, comparing inner and outer subsectors. An understanding of these fields, along with the electron drift properties of P10, allows one to predict the sensitivity of $Z'_{\mathrm{d,in}}$ and $Z'_{\mathrm{d,out}}$ to various TPC parameters.

TPC Anode Plane Regions: 1998–1999 Operating Parameters

The STAR TPC has been operating with P10 (90% Ar, 10% CH_4 by volume) at ∼4 mbar above the ambient atmospheric pressure. Calculated electron drift properties for P10 are available from the MAGBOLTZ code [Biagi, 1995], interfaced to GARFIELD [Veenhof, 1995] for use in gas detector simulations. As a function of "reduced field" (E/P, electric field divided by pressure), drift velocity V_{drift} is shown in Fig. 1 for several alignments of the electric and magnetic fields.

In the drift region of the STAR TPC, the electric field $\vec{E_{\mathrm{drift}}}$ is nearly aligned with the magnetic field $\vec{B_{\mathrm{drift}}}$, and large enough ($E/P \approx 0.19$) that V_{drift} is beyond saturation ($dV_{\mathrm{drift}}/dE_{\mathrm{drift}} < 0$). Not operating at saturation allows active regulation of drift time with E_{drift}, allowing compensation for non-ideal factors, such as variations in the argon-methane ratio or low levels of contaminents.

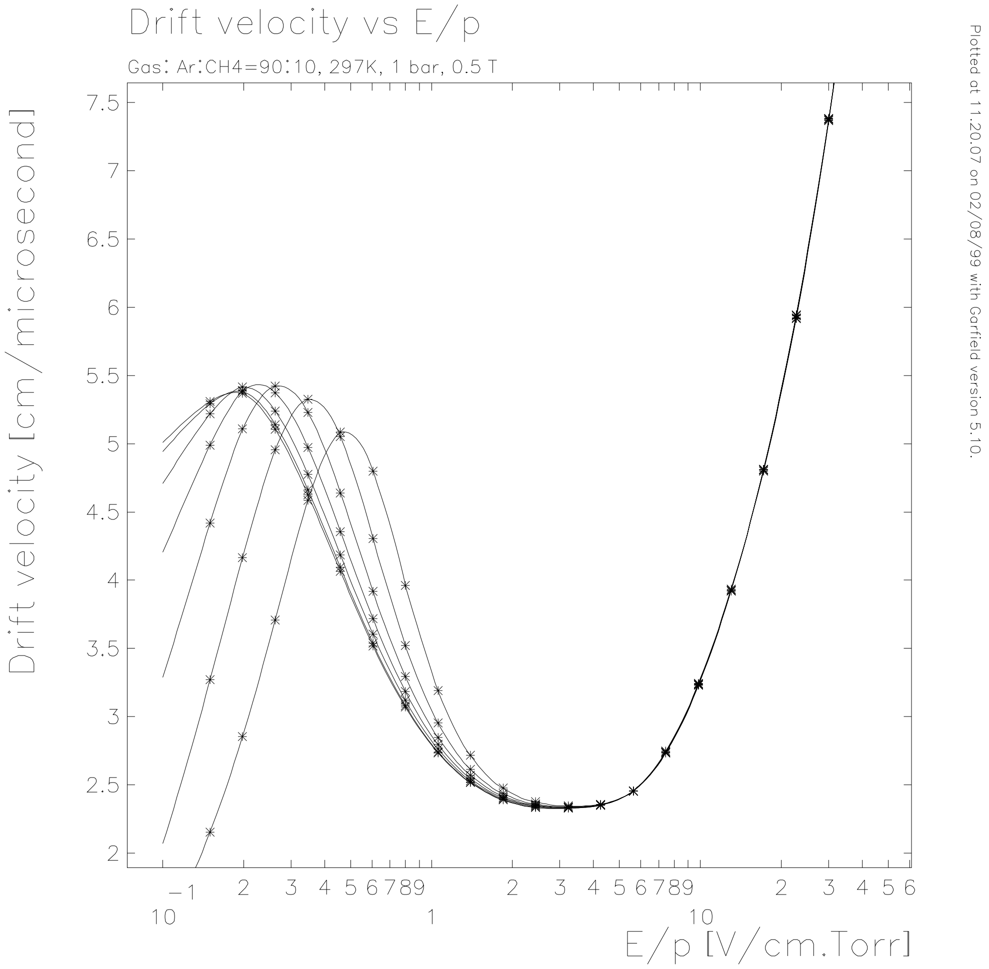

Figure 1: Drift velocity of electrons in P10 as a function of E/P for $\vec{E}$, $\vec{B}$ field alignments of 0–90° (from left to right), at 15° intervals.

The TPC design has been discussed elsewhere, but, for convenience, a sketch emphasizing its anode-wire regions appears in Fig. 2. The relevant parameters for the 1998–1999 running periods, derived by Eric Hjort [Hjort, 1997], are summarized in Table 1. The gating grid potential in Table 1 is for the open state; the closed-state potentials are presently symmetric, at -75 V and -130 V.

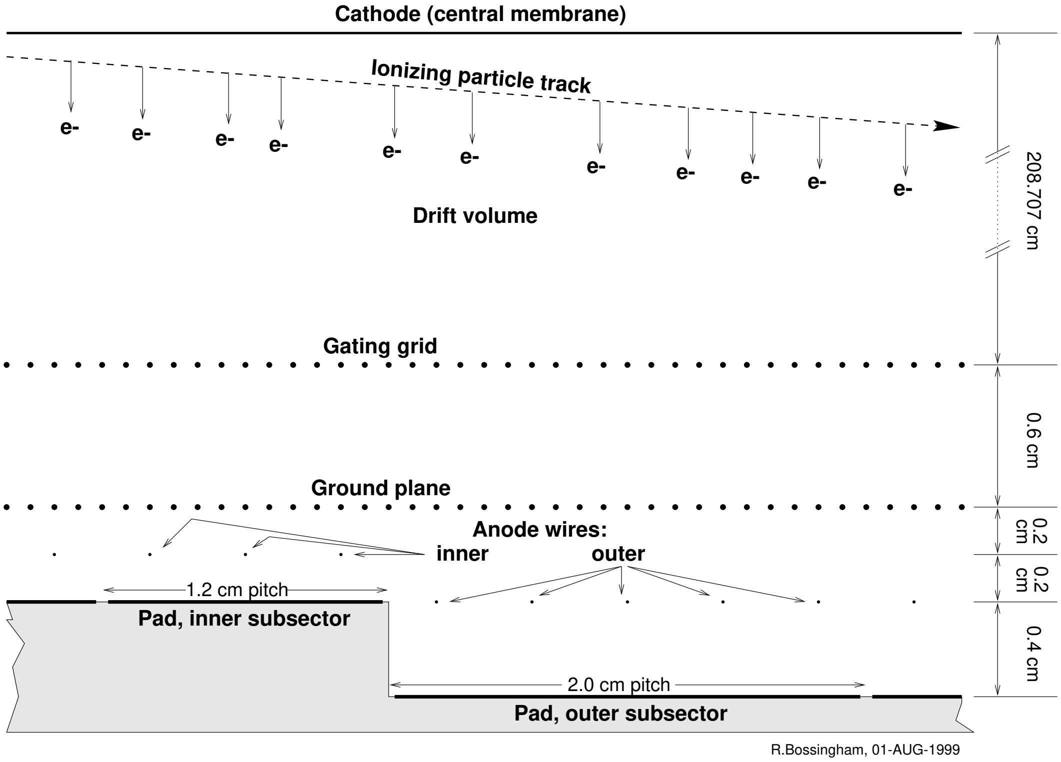

Figure 2: The relative geometric distances to the anode wires in the inner and outer subsectors are shown here. For clarity, the wire diameters are drawn larger than scale, and the buffer regions and gap at the subsector edges have been omitted.

Equipotential lines in the anode-plane regions, shown in Fig. 3, indicate that the uniform drift field region extends from the cathode to the gating grid, almost. This is followed by a higher field, still nearly uniform, to the ground wire plane. The field increases from there to the anode wires.

The gross electron-drift features, shown in Fig. 4, are unsurprising: isochrones roughly parallel equipotential lines, and drift lines are compressed into four drift channels that converge at the anode wire. Drift through the outermost pair of channels requires an extra 0.020–0.030 μs, reflecting the longer drift paths. This effect has been studied in detail elsewhere. [Betts, 1996]

Electron Drift Times near the Anode Plane

The field is nearly uniform and constant 0.2 cm or more before the gating grid, so one can simulate the drift of ionization from there to the anode wires to estimate the difference between the inner- and outer-subsector drift times. The results appear in Fig. 5, predicting that drift in the outer subsector requires an additional 0.083 μs.

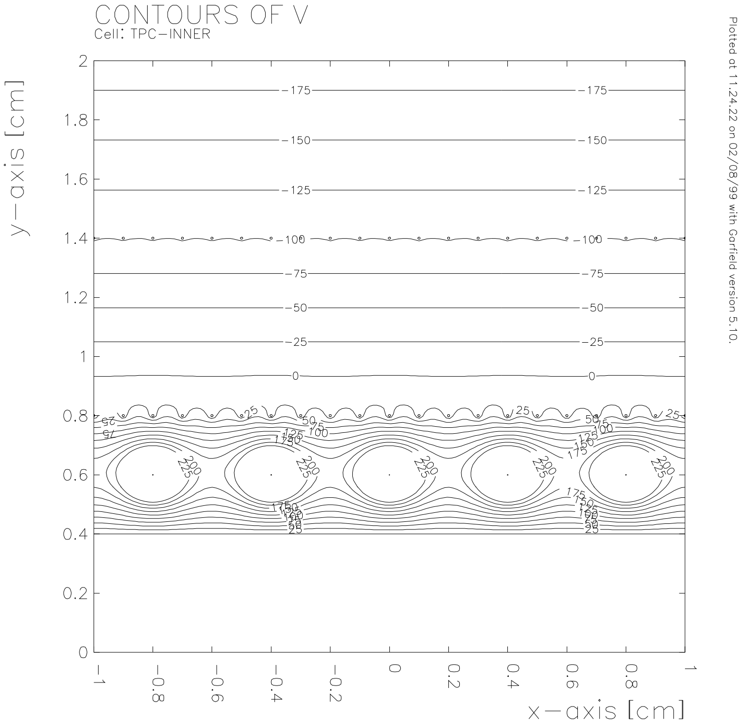

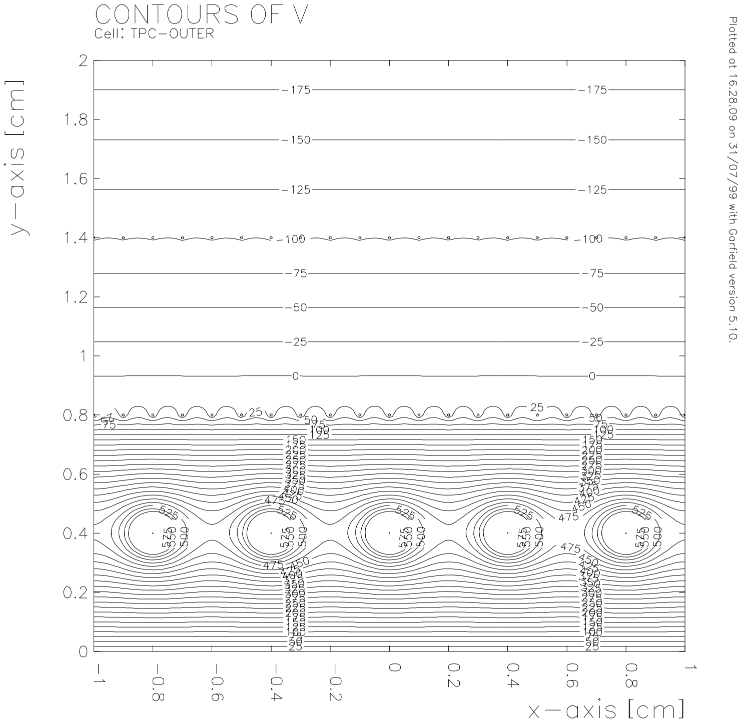

Figure 3: Equipotentials from drift volume to pad plane for the inner subsector (top) and outer subsector (bottom). Each plot is for a slice with five anode wires; note that these coordinates ($y = 0.4$ cm and $y = 0.0$ cm are Garfield-related, rather than global TPC coordinates.

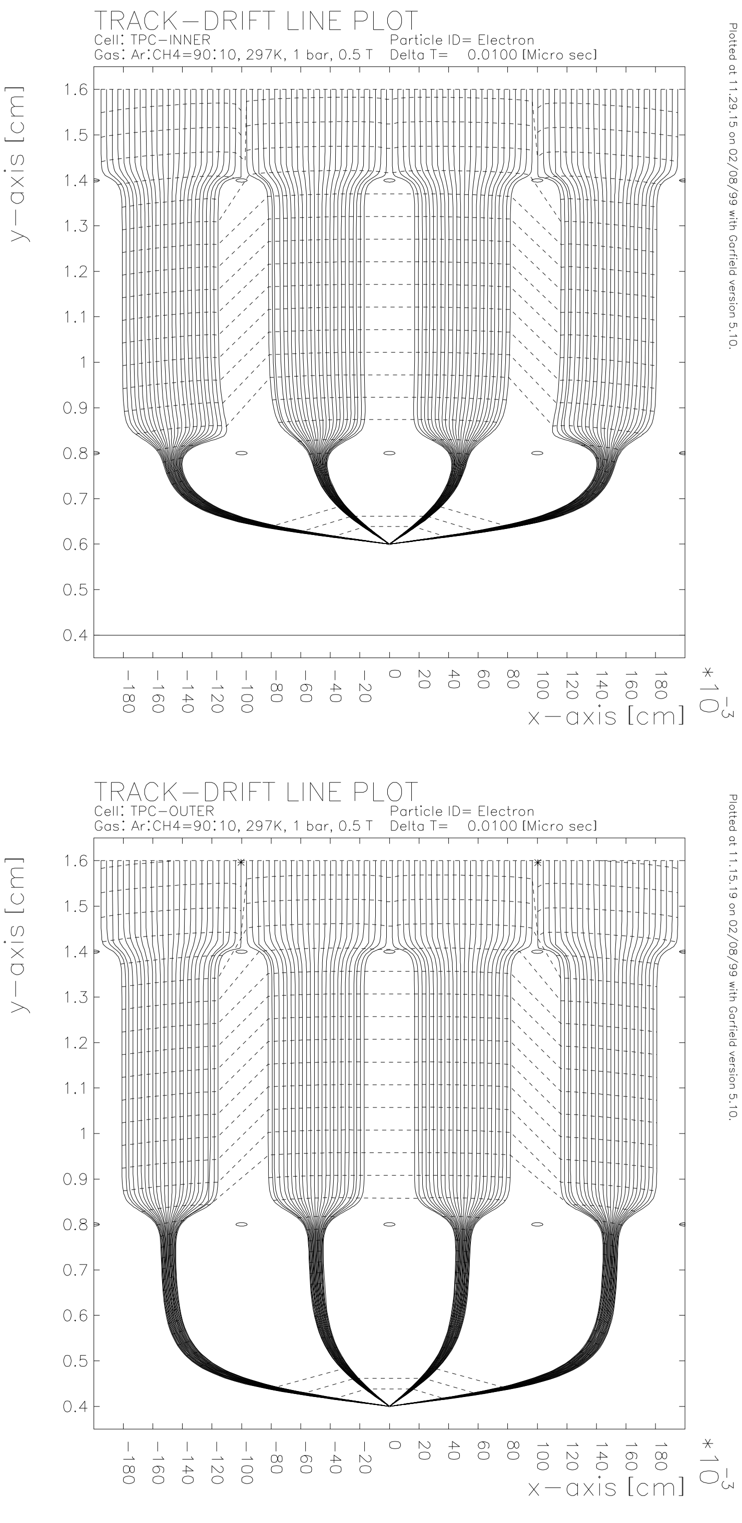

Figure 4: Electron drift past the gating grid and ground wires to the anode wires for the inner subsector (top) and outer subsector (bottom); isochrones are spaced at 0.010 μs.

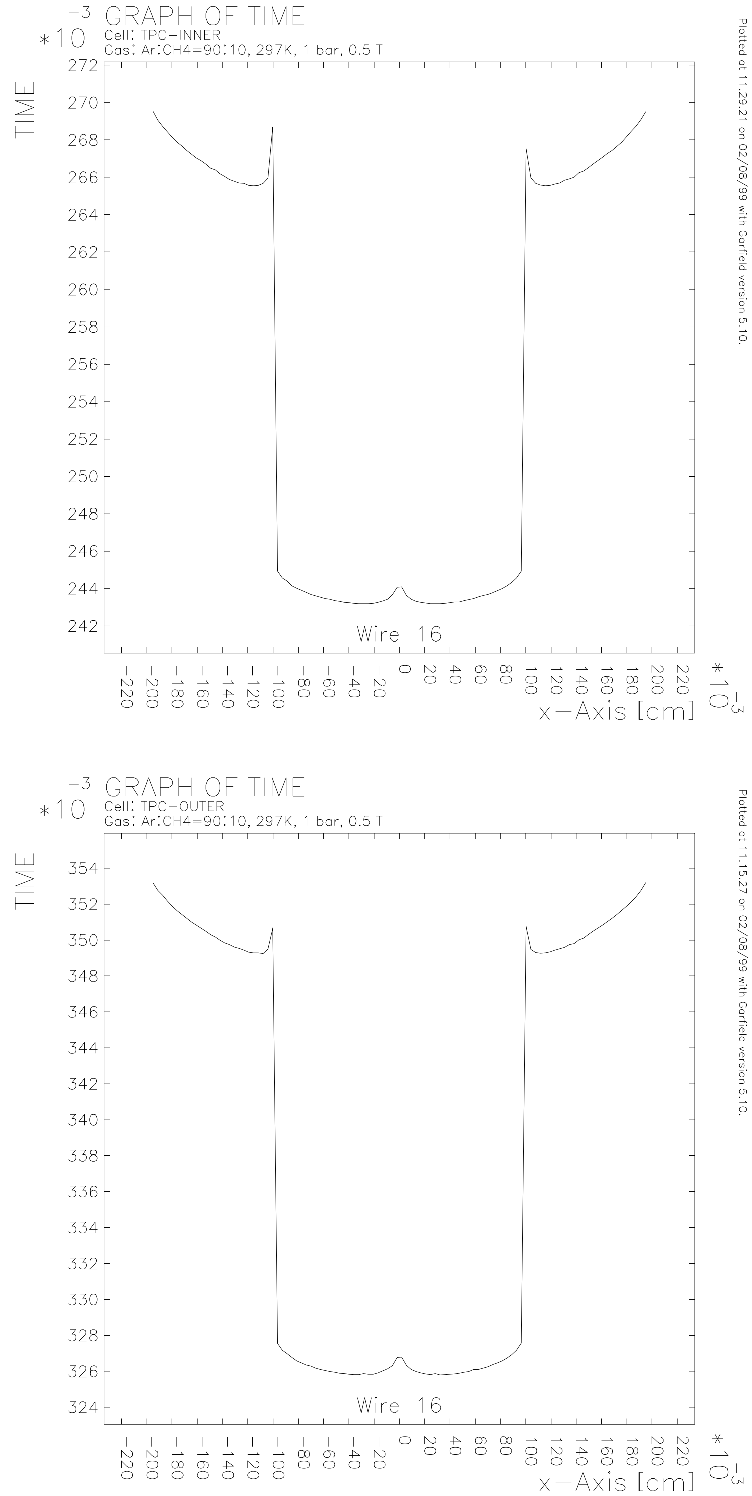

Figure 5: Times for electrons to drift from a track 0.2 cm before the gating grid to an anode wire in an inner subsector (top) and an outer subsector (bottom). Times are in microseconds.

	Z (cm)	Wire Diameter (cm)	Potential (V)
Cathode	0.00	-	-31000.0
Gating grid	$\pm$208.7	0.0075	-102.5
Ground wires	$\pm$209.3	0.0075	0.0
Inner:			
Anode wires	$\pm$209.5	0.0020	1150.0
Pad plane	$\pm$209.7	-	-1.5
Outer:			
Anode wires	$\pm$209.7	0.0020	1400.0
Pad plane	$\pm$210.1	-	-1.5

Table 1: Nominal TPC parameters for 1998–1999.

At the nominal TPC drift field (148.05 V/cm) with $\vec{E}_{\rm drift}$ and $\vec{B}_{\rm drift}$ parallel, MAGBOLTZ predicts $V_{\rm drift} = 5.396$ cm/μs. This is a bit below the $\sim$5.506 cm/μs value seen in the STAR TPC, but the calculation here will be internally consistent and give correct values for $Z'_{\rm d,in}$ and $Z'_{\rm d,out}$, if the ratio of real to calculated drift velocity is constant.

The drift numbers are summarized in Table 2, showing the prediction that $Z'_{\rm d,out} - Z'_{\rm d,in} = 0.47$ cm for the alignment of the inner and outer subsectors—as opposed to the $Z_{\rm d,out} - Z_{\rm d,in} = 0.20$ cm naively expected.

	$Z_{\rm d} - Z_0$ (cm)	$t_{\rm d} - t_0$ (μs)	$(t_{\rm d} - t_0) \times V_{\rm drift}$ (cm)	$Z'_{\rm d} - Z_{\rm d}$ (cm)
Inner	1.0	0.2515	1.357	0.357
Outer	1.2	0.3385	1.827	0.627
Outer-Inner	0.2	0.0870	0.470	0.270

Table 2: Summary of the drift time results from GARFIELD.

Experimental Values

The first alignment [Long, 1997] of inner and outer TPC subsectors using 1997 cosmic-ray data and a χ^2-minimization approach obtained $Z'_{\rm d,out} - Z'_{\rm d,in} = 0.35$ cm. The TPC operating parameters were different (no magnetic field, slightly different voltages), but, as discussed below, the fitted value should not be affected significantly.

Similar results are found from the 1999 data, comparing average drift times from the central membrane to the anode wires for inner and outer subsectors. The input data are:

$$\text{Total drift time [Howard Wieman]} : T_{\rm d} = 38.2\ \mu\text{s}$$

$$\text{ADC sampling period} : \Delta T_{\rm bucket} = 0.10703\ \mu\text{s}$$

$$\text{Drift time difference} : T'_{\mathrm{d,out}} - T'_{\mathrm{d,in}} = 0.6 \Delta Z_{\mathrm{bucket}}$$

$$\text{From the discussion above} : Z'_{\mathrm{d,out}} - Z_{\mathrm{d,out}} = 0.63 \ \ \mathrm{cm}$$

$$\text{From the data} : Z'_{\mathrm{d,out}} - Z'_{\mathrm{d,in}} = 0.6\, \Delta Z_{\mathrm{bucket}}$$

From these values, one finds:

$$Z'_{\mathrm{d,out}} = (209.7 + 0.63) \ \ \mathrm{cm} = 210.33 \ \ \mathrm{cm}$$

$$V_{\mathrm{drift}} = Z'_{\mathrm{d,out}}/T_{\mathrm{drift}} = (210.33 \ \ \mathrm{cm})/(38.2 \ \ \mu\mathrm{s}) = 5.506 \ \ \mathrm{cm}/\mu\mathrm{s}$$

$$\Delta Z_{\mathrm{bucket}} = \Delta T_{\mathrm{bucket}} \cdot V_{\mathrm{drift}} = (0.10703 \ \ \mu\mathrm{s}) \cdot (5.506 \ \ \mathrm{cm}/\mu\mathrm{s}) = 0.5893 \ \ \mathrm{cm}$$

$$Z'_{\mathrm{d,out}} - Z'_{\mathrm{d,in}} = 0.6\, \Delta Z_{\mathrm{bucket}} = 0.6 \cdot 0.5893 \ \ \mathrm{cm} = 0.35 \ \ \mathrm{cm}$$

Therefore, the 1999 and 1997 calibrations both produce $Z'_{\mathrm{d,out}} - Z'_{\mathrm{d,in}} = 0.35$ cm—in contrast to the GARFIELD/MAGBOLTZ prediction of 0.45 cm.

Sensitivity to some Variable TPC Parameters

As a practical issue for calibrations, one needs an estimate of the sensitivity of calibration values to operational variables; such estimates, based on GARFIELD/MAGBOLTZ, are shown in Table 3.

	$\Delta t_{\mathrm{GG}\rightarrow\mathrm{anode}}$ (μs) for Parameter Change				
	$B \rightarrow 0$	V_{anode}: +100 V	$V_{\mathrm{gatedgrid}}$: -50 V	E_{drift}: +50 V/cm	P: -50 Torr
Inner	~0	+0.0010	+0.0155	+0.0005	+0.0030
Outer	~0	+0.0015	+0.0150	+0.0005	+0.0035
Drift region, 1 cm	~0	~0	~0	+0.0090	+0.0005

Table 3: Estimated drift time sensitivity to parameter changes; the remaining parameters are the nominal 1998–1999 values.

As it happens, $Z'_{\mathrm{d,out}}$ and $Z'_{\mathrm{d,in}}$ are insensitive to variations of the magnetic-field strength along the electron drift paths: either $\vec{B}$ is nearly parallel to the drift velocity, or E/P is so large that the drift is no longer sensitive to $\vec{B}$. The calculated drift times change no more than a fraction of a nanosecond as B varies from zero and 0.5 T.

Drift times are also insensitive to the anode wire potential because, over most of the volume where E is sensitive to it, dV_{drift}/dE is small. In contrast, dV_{drift}/dE is large between the gating grid and ground wires, so the drift time is sensitive to the gating grid potential, but the effect on the inner and outer subsectors is nearly identical.

Increasing E_{drift} by +50 V/cm reduces V_{drift} as expected, but there is little field leakage past the gating grid and drift times from there to the anode wire are only slightly affected. Recalling that drift velocity is a function of E/P, such an increase in E_{drift} is equivalent to a pressure drop of 192 Torr in the drift region. However, pressure drops affect E/P over the full TPC, so drift times past the gating grid are more changed by $\Delta P = -50$ Torr than by a $E_{\mathrm{drift}} = +50$ V/cm in the drift volume alone.

Review of Anode-Area Details

The 1998–1999 operating voltages [Hjort, 1997] in Table 1 translate into the nominal fields in Table 4. The field in the drift volume was calculated by the Eric Hjort's applet; the other values are from GARFIELD, after the parameters were tuned to reproduce the field in the drift volume.

	Field (V/cm)	ΔZ (cm)	V_{drift} (cm/μs)
Drift volume	148.05	208.7	5.396
GG to gnd. wires	216.76	0.6	4.969

Table 4: Calculated TPC values for nominal 1998–1999 parameters.

The calculated E-field contours near the anode wire, up to the ground-wire plane, are shown in Fig. 6. An interesting feature of much of the region is that $E/P \sim 2$, for which V_{drift} is insensitive to E¶.

The electron drift lines in Fig. 7 show the regions of the field usually sampled. Note that the angle of the drift lines to the TPC axis (unfortunately labeled y in the GARFIELD plots) never exceeds $\sim 60°$.

More Details of the TPC Electric Field

In discussing the electron drift time, it is helpful to know the E field in the transition regions near the ground-wire plane and gating grid; these are shown in Figs. 8, 9, respectively.

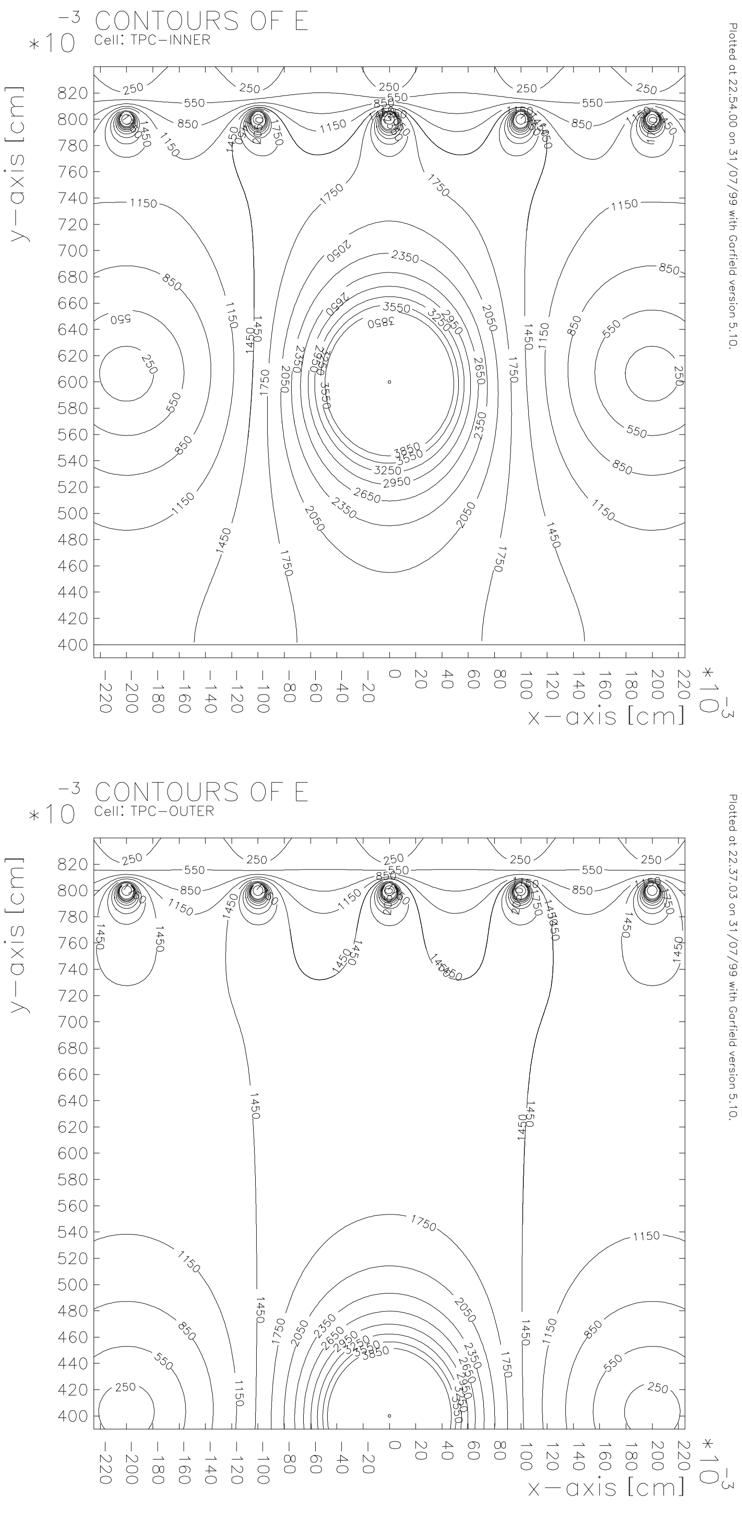

Figure 6: Electric field contours from ground wires to pad plane in the inner subsector (top) and from ground to anode wires in the outer subsector (bottom).

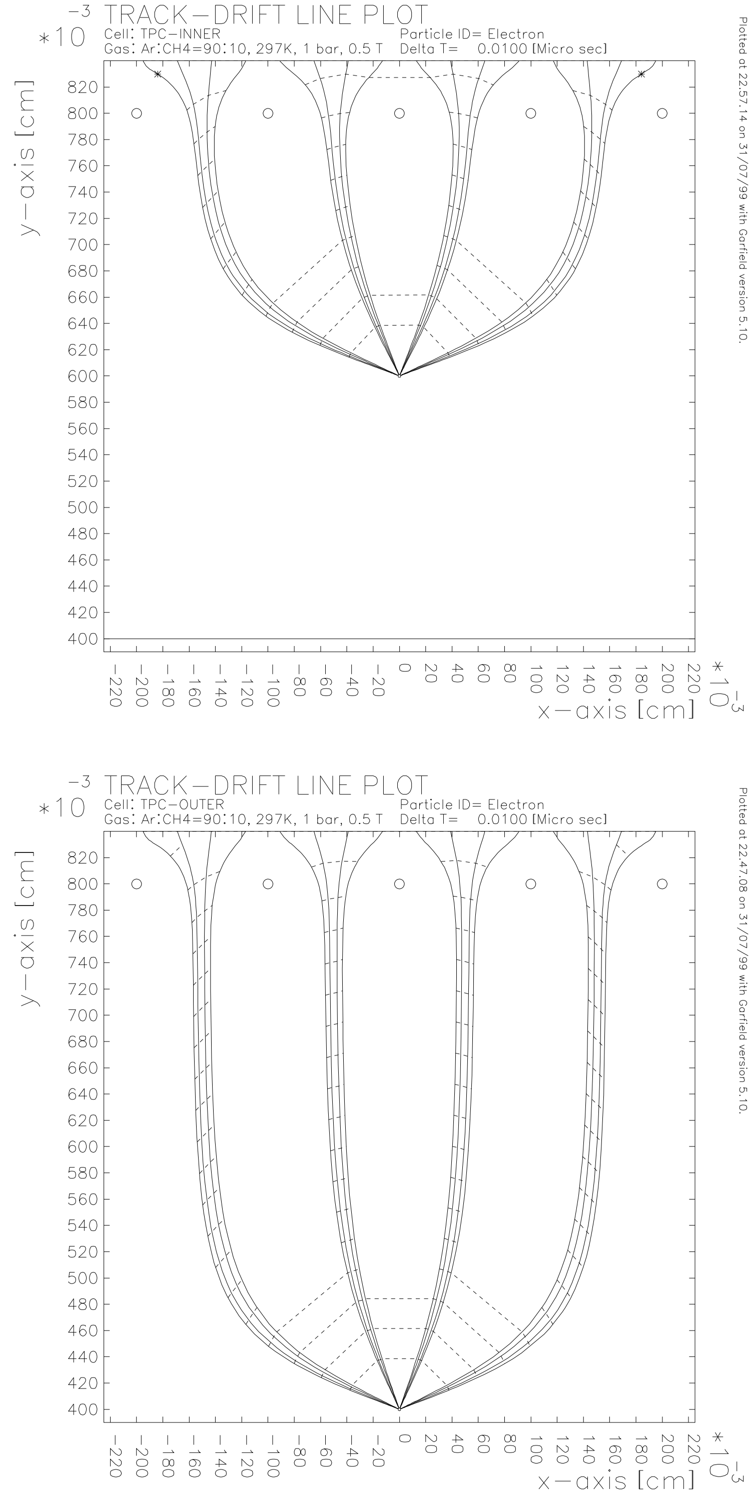

Figure 7: Electron drift to the anode wires in the inner subsector (top) and outer subsector (bottom). Isochrone spacing is 0.010 μs; note the extra 0.020–0.030 μs that electrons in the far channels require.

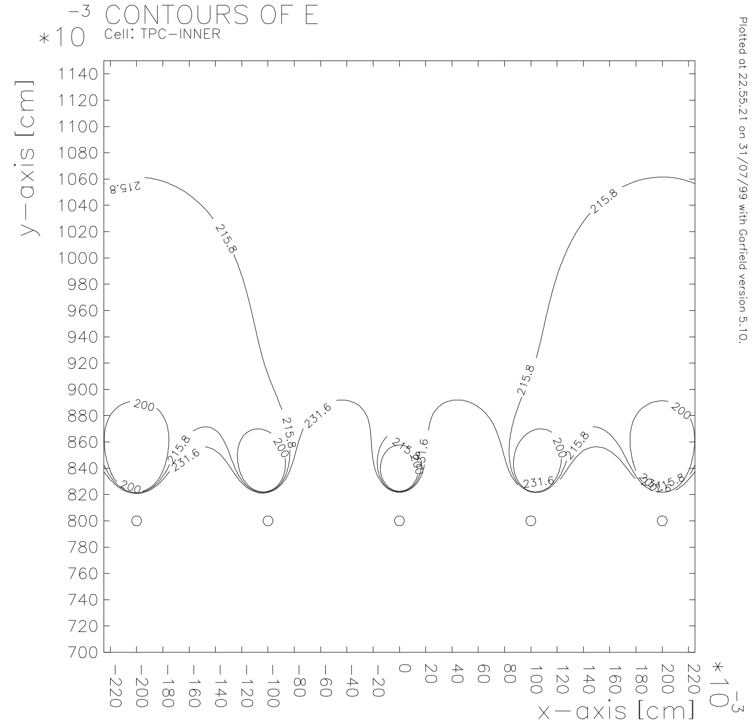

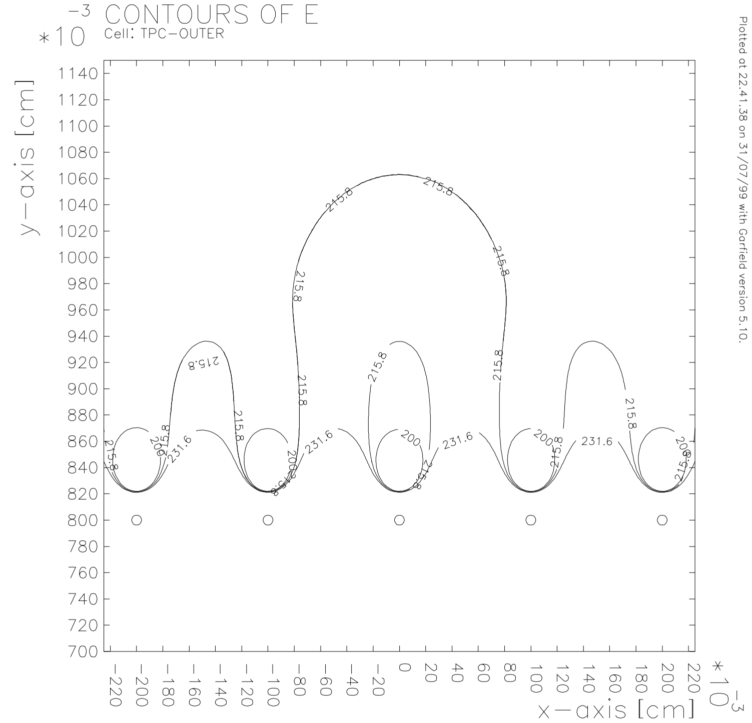

Figure 8: Electric field contours for an anode-wire cell in the inner subsector (top) and outer subsector (bottom); in both, the effect of the anode wire (below lower axes of plots) heals out a couple of millimeters past the ground-wire plane.

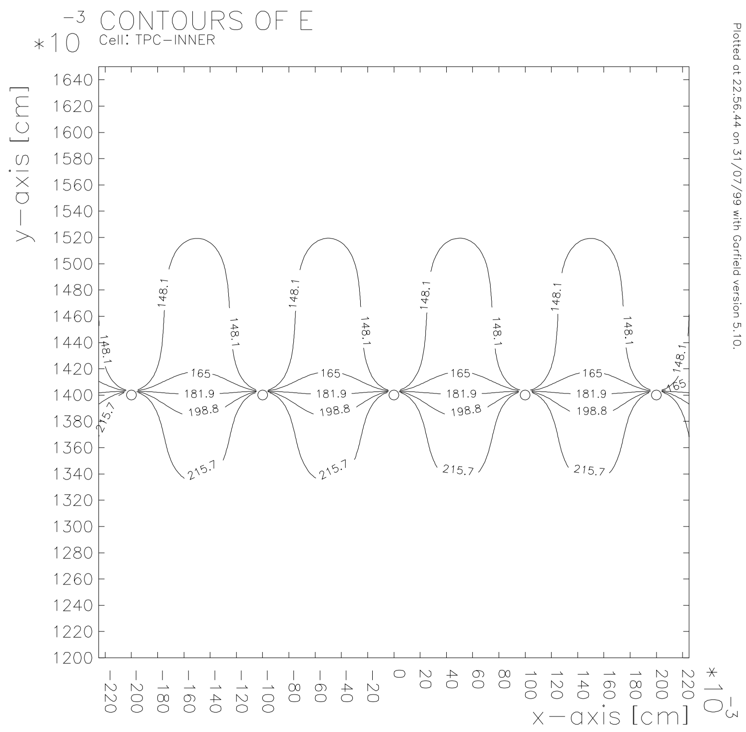

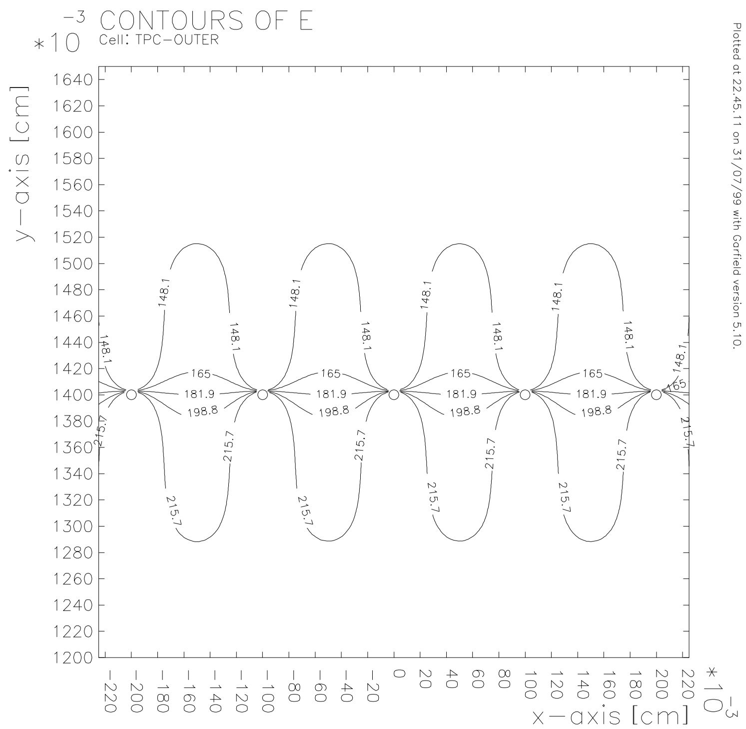

Figure 9: Electric field contours in the inner subsector (top) and outer subsector (bottom), showing the transition from the drift region, at top, across the gating grid.

P10 Drift Properties

Figure 10 shows V_{drift} in P10 vs. E/P on a linear scale. The main drift region of the TPC corresponds to $E/P \sim 0.19$ V/cm-Torr, slightly to the right of the saturation peak for $\vec{E}$ and $\vec{B}$ parallel. In the higher-field region within $\sim 500\ \mu$m of the anode wires, V_{drift} increases with E/P linearly, or almost as the inverse of the distance to the wire. Away from the anode wires, the log scale in the lower plot of Fig. 11 is more appropriate, showing that V_{drift} is near constant for $E/P \sim 1.5$–5. Most of the shift of the effective detection planes occurs in this region.

For calibration purposes, another important property of P10 is the Lorenz angle shown in Fig. 12, which allows one to estimate the size of the $E \times B$ effect near the anode wires. Finally, for completeness, plots of the Townsend and attachment coefficients appear in Fig. 13.

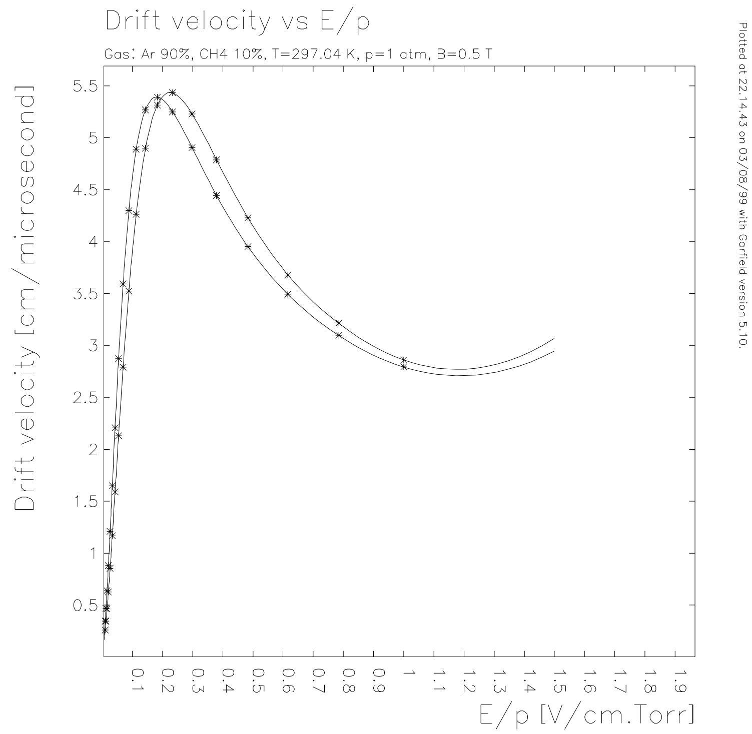

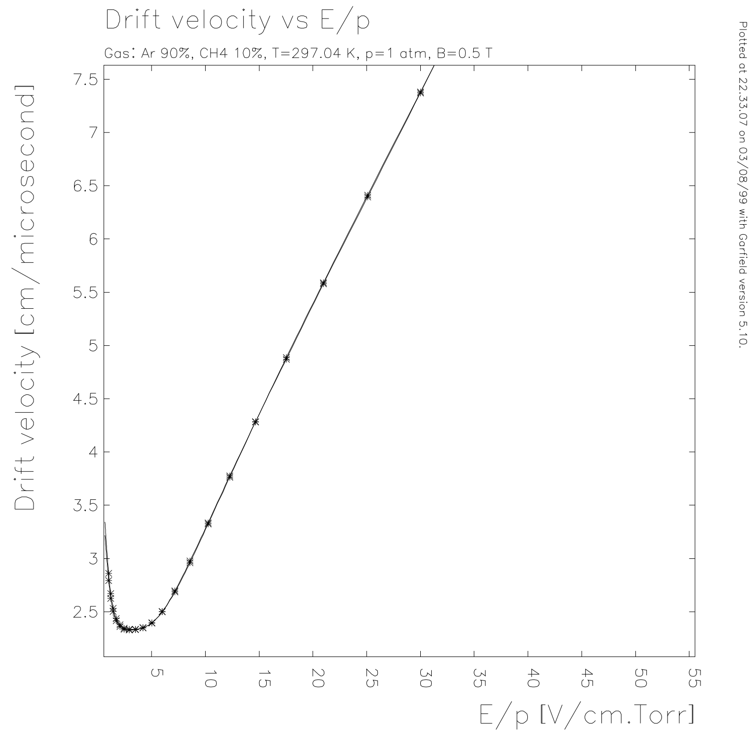

Figure 10: Electron drift velocity in P10 in low fields (top) and higher fields (bottom). The left-hand curve is for parallel $\vec{E}$ and $\vec{B}$ fields; for the right-hand curve (merged at high E/P) they are at 45°.

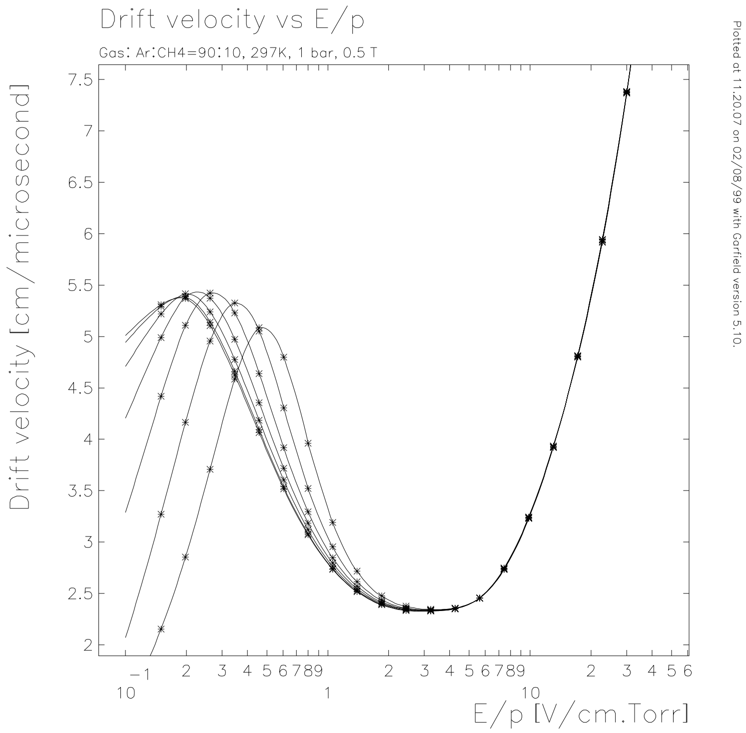

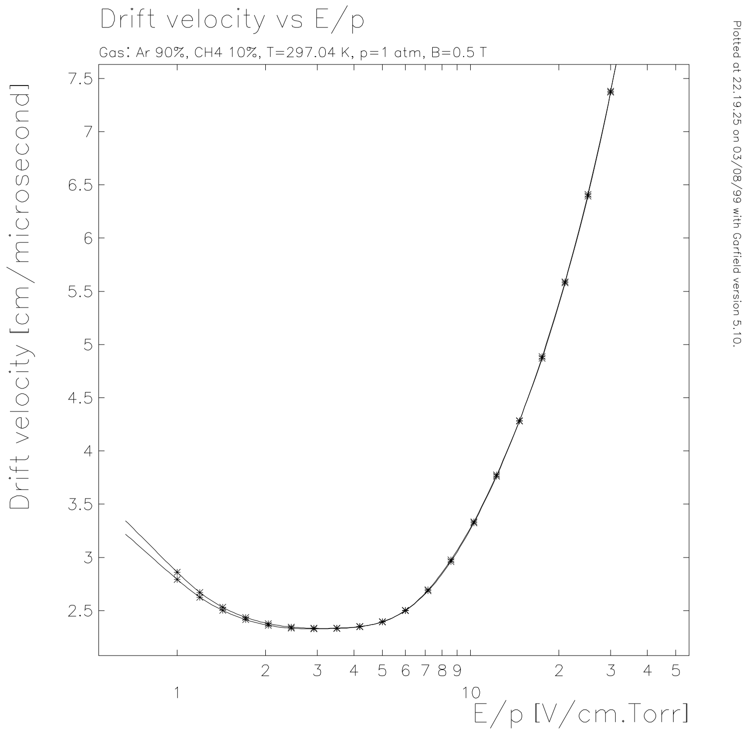

Figure 11: Drift velocity in P10: overall (top) and in the higher-field region only (bottom). The low drift velocities for $E/P \sim 2$ cause most of the "effective detection plane" shift.

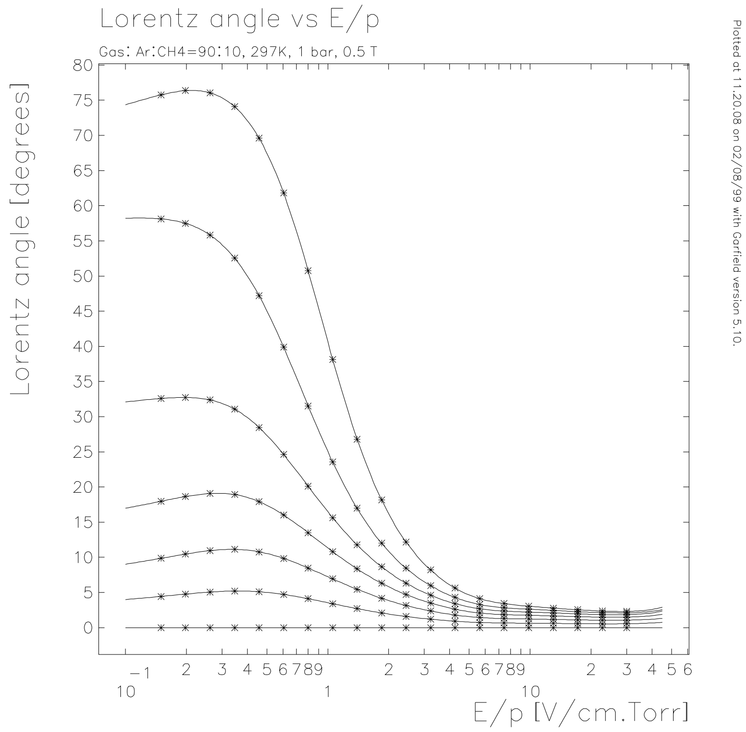

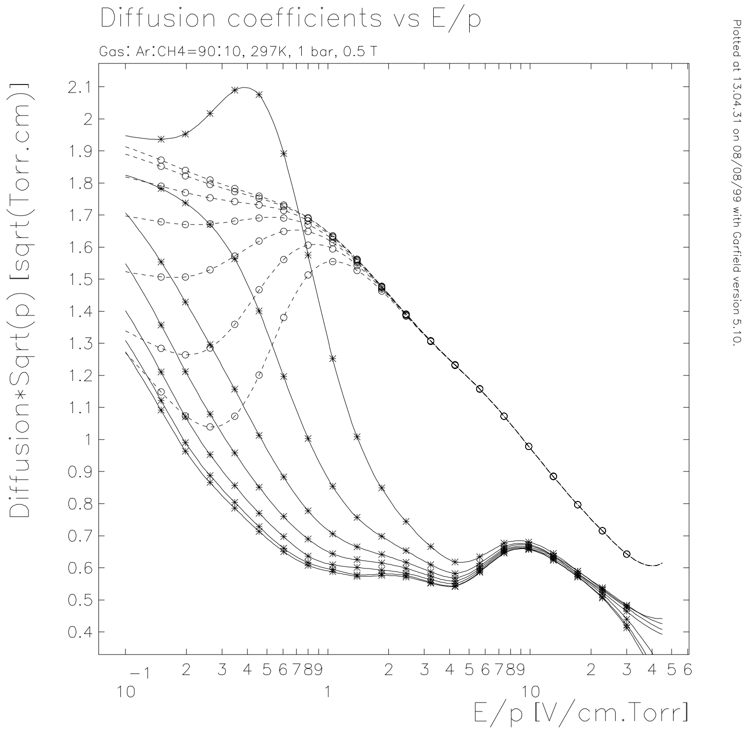

Figure 12: Lorentz angles (top) and diffusion (bottom) in P10 at 297K and 1 bar, with a 0.5-T $\vec{B}$-field at 0°, 15°, 30°, 45°, 60°, 75° and 90° to $\vec{E}$. For increasing angle: Lorentz angles and transverse diffusion (*'s) increase; longitudinal diffusion (open circles) decreases.

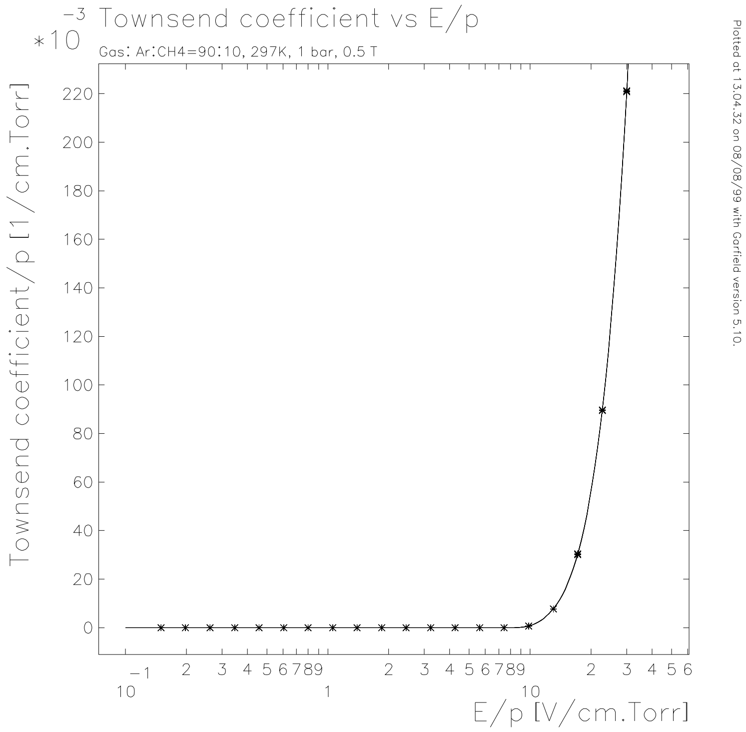

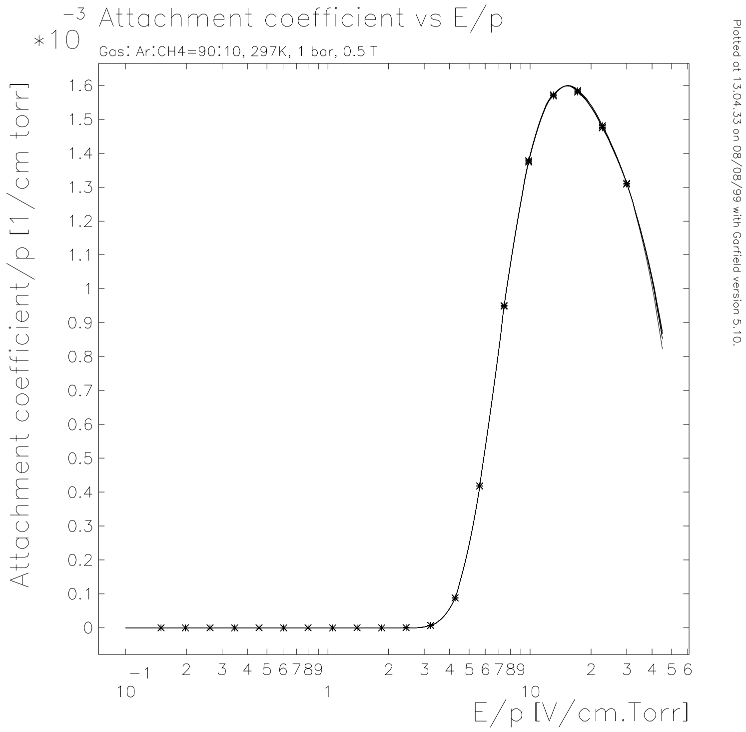

Figure 13: Townsend coefficients (top) and attachment coefficients (bottom) in P10 at 297K and 1 bar.

Garfield Simulation Details

Some basic GARFIELD scripts, used to define the TPC gas and electrostatics for the simulations, are given below. These were used with GARFIELD V5.10, interfaced to MAGBOLTZ V1.08. They will not necessarily work with earlier versions of the code. (The converse is also true: V4 scripts do not work with GARFIELD V5.) These V5 scripts were derived from a generalized V5 script by Wayne Betts.)

It takes significant time (~15 minutes on rcf.rhic.bnl.gov) to calculate the gas properties. This is usually done once for a given gas definition and saved for future use. GARFIELD allows the user to adjust several parameters, and this must sometimes be done carefully to prevent problems. Even so, the calculations do not necessarily converge for all points; dozens of warnings issued from the run below, mostly related to the diffusion calculations. The cluster calculation definitely did not work as expected, and would have to be reworked before the cluster aspects of the gas file could be trusted.

```
&MAGNETIC
 COMP 0.0 0.5 0.0 T
&GAS
 OPTION GAS-PLOT
 TEMPERATURE 297.04
 PRESSURE 760.
 PARAMETER MEAN 30.
 CLUSTER  EXP(-((N-3)/2)**2) N 10
 MAGBOLTZ ARGON 0.90 METHANE 0.10 E/P-RANGE 0.15 30. ANGLE-RANGE 0. 90. ...
          N-ANGLE 7 MOBILITY 1.87E-6
 WRITE DATASET 'P10_5KG_297K_760T.DAT' REMARK "P10, 5 kG, 297.04K, 1 bar"
&STOP
```

The drift simulations do not use mock up the entire TPC, but only use enough wires for the fields near the center wires to approach the infinite case close to the anode planes. Similarly, the cathode plane is not placed at the real position, but only a few centimeters away from the wire planes; it's potential is set to reproduce the correct drift field.

Also, GARFIELD is not always numerically stable. It is often necessary to adjust ranges, etc. empirically to get "good" plots. One frequently has to customize the code itself—either to adjust array sizes or algorithms—but the only the distribution code was used for this Note. Unfortunately, GARFIELD plots are often not of publication quality, and many parameters are hard-wired in the code; again, one would have to hack and recompile the code to fix this.

Typical scripts for inner, then outer, subsector simulations follow:

```
&CELL
 CELL-IDENTIFIER TPC-INNER
 PLANE   Y   0.4   V    -1.5
 PLANE   Y   3.4   V  -397.0422
 ROWS
 S  31  0.0020   -6.0+I*0.4   0.6000   1150.0
 F 125  0.0075   -6.2+I*0.1   0.8000      0.0
 F 125  0.0075   -6.2+I*0.1   1.4000   -102.5
&MAGNETIC
 COMP 0.0 0.5 0.0 T
&GAS
 GET 'P10_5KG_297K_760T.DAT'
&FIELD
 AREA -1.0 0.0 1.0 2.0
 PLOT CONTOUR V RANGE -175.  225. N 16
&DRIFT
 LINES 104
 AREA  -0.200  0.35  0.200  1.65
 TRACK -0.195  1.60  0.195  1.60
 DRIFT TRACK FUNCTION-GRAPH TIME CONTOUR 0.010

&CELL
 CELL-IDENTIFIER TPC-OUTER
 PLANE   Y   0.0   V    -1.5
 PLANE   Y   3.4   V  -397.0422
 ROWS
 S  31  0.0020   -6.0+I*0.4   0.4000   1400.0
 F 125  0.0075   -6.2+I*0.1   0.8000      0.0
 F 125  0.0075   -6.2+I*0.1   1.4000   -102.5
&MAGNETIC
 COMP 0.0 0.5 0.0 T
&GAS
 GET 'P10_5KG_297K_760T.DAT'
&FIELD
 AREA -1.0 0.0 1.0 2.0
 PLOT CONTOUR V RANGE -175.  575. N 30
&DRIFT
 LINES 104
 AREA  -0.200  0.35  0.200  1.65
 TRACK -0.195  1.60  0.195  1.60
 DRIFT TRACK FUNCTION-GRAPH TIME CONTOUR 0.010
```

References

Betts, 1996: W. Betts, W. Gong, E. Hjort and H. Wieman, Star Note SN0263, "Studies of Several Wire and Pad Geometries for the STAR TPC," 1996.

Biagi, 1995: Steve Biagi, MAGBOLTZ interface to /GARFIELD; V1.08, April 1995.

Hjort, 1997: Java applet by Eric Hjort; available online at `http://www.star.bnl.gov/STAR/html/tpc_l/hard/tpcrings/page6.html`.

Long, 1997: Hui Long, preliminary alignment.

Veenhof, 1995: Rob Veenhof, GARFIELD 5.10, May 1995.